ADVANCED FUNCTIONAL MATERIALS
www.afm-journal.de

Check for updates

Disassembling Silicene from Native Substrate and Transferring onto an Arbitrary Target Substrate

Christian Martella, Gabriele Faraone, Muhammad Hasibul Alam, Deepyanti Taneja, Li Tao, Guido Scavia, Emiliano Bonera, Carlo Grazianetti, Deji Akinwande,* and Alessandro Molle**

Here, two novel approaches for disassembling epitaxial silicene from the native substrate and transferring onto arbitrary target substrates are presented. From the processing perspective, the two methodologies open up a new route for handling silicene, and in general any epitaxial Xene, in view of establishing reliable process flows for the development of a Xene-based nanotechnology. Integration of silicene in a back-gated controlled device architecture is demonstrated and the built up of unique multi-stack heterostructures between silicene, but potentially every Xene, and other technological relevant materials, like transparent conductive oxides and transition metal dichalcogenides is shown.

1. Introduction

2D materials, from graphene to transition metal dichalcogenides (TMDs) and more, have opened up disruptive opportunities in the evolution of nanotechnology with their exotic physics.[1–4] This scenario has been paralleled by a concomitant effort to process these 2D materials by means of device integration schemes aiming at reinforcing production scalability and, at the same time, at developing procedural steps for their transfer and handling. These goals in the case of Xenes, namely the 2D honeycomb-like form of mono-elemental materials, are a major undertaking.[5] Indeed, the dawn of a Xene-based technology is hindered by non-trivial challenges in post-deposition processing.[6,7] Xenes grown in ultra-high-vacuum conditions are, in all likelihood, affected by air-stability issues when manipulated under ambient conditions.[8] In addition, Xenes deposited by epitaxial techniques have to deal with the choice of a proper supporting substrate, which may represent concomitantly both the key player for the growth and the limiting factor for the integration into devices. A smart choice of the growth-substrate is, therefore, the first step toward the successful development of operating procedures for the device fabrication process.[7,9]

However, most of the epitaxial Xenes, including silicene, germanene, stanene, borophene, blue-phosphorene, and antimonene, forcedly grow on single crystal (111)-terminated metal substrates like noble metals.[10–14] Opting for sample transfer procedures, the use of crystalline silver or gold thin films on mica as templates for the Xene epitaxy, instead of expensive bulk metals, facilitated the realization of delamination schemes like "silicene encapsulated delamination with native electrode" (SEDNE)[7] and then the "universal X-ene encapsulation, decoupling and operation" (UXEDO) processes.[15] Both these approaches took advantage of the mica cleavability, by means of its mechanical or chemical delamination, and of the in situ encapsulation of the Xene to set milestones on the roadmap toward a Xene-based device technology. Tao et al.[7] using the SEDNE approach pioneered a silicene transistor operating at room temperature. Grazianetti et al.[15] using the UXEDO approach extended the methodologies of the SEDNE to epitaxial blue-phosphorene, thus demonstrating the universality of the approach.

Here, we discuss two approaches for the manipulation of an encapsulated Xene. We take the epitaxial silicene as a paradigmatic Xene case to show how it can be disassembled from the native substrate, and subsequently transferred onto an arbitrary target substrate.[16] We will refer to the first approach

Dr. C. Martella, G. Faraone, Dr. C. Grazianetti, Dr. A. Molle
CNR-IMM
unit of Agrate Brianza
via C. Olivetti 2, Agrate Brianza, MB 20864, Italy
E-mail: alessandro.molle@mdm.imm.cnr.it

G. Faraone, Prof. E. Bonera
Dipartimento di Scienza dei Materiali
Universita' di Milano-Bicocca
Via Cozzi 53, Milano I-20125, Italy

Dr. Md. H. Alam, Dr. D. Taneja, Prof. D. Akinwande
Microelectronics Research Centre
The University of Texas at Austin
Austin, TX 78758, USA
E-mail: deji@ece.utexas.edu

Prof. L. Tao
School of Materials Science and Engineering
Southeast University
2 Southeast University Road, Nanjing 211189, China
E-mail: tao@seu.edu.cn

Dr. G. Scavia
CNR-SCITEC
via A. Corti 12, Milano 20133, Italy

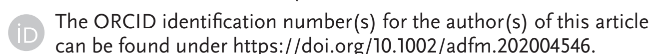
The ORCID identification number(s) for the author(s) of this article can be found under https://doi.org/10.1002/adfm.202004546.

© 2020 The Authors. Published by Wiley-VCH GmbH. This is an open access article under the terms of the Creative Commons Attribution License, which permits use, distribution and reproduction in any medium, provided the original work is properly cited.

DOI: 10.1002/adfm.202004546

as seamless SEDNE (s-SEDNE). In the original SEDNE process, after the mica delamination, the membrane made by the silicene sandwiched between the capping layer and the metal substrate was place in contact with the target substrate. Several vacuum annealing steps were required to form a smooth interface and a firm contact between the capping layer and the back gate-oxide of the target substrate. Subsequently, the native metal substrate was patterned by e-beam lithography obtaining the electrical contacts. At variance with the SEDNE, the s-SEDNE involves an initial deposition step of a high-k Al_2O_3/Au (gate dielectric and gate electrode) on top of the thin capping layer. This not only improves the mechanical strength of the delaminated membrane, but in addition allows for seamless dielectric gating control on silicene when integrated into a back-gated device configuration. The second approach, called transfer-UXEDO (t-UXEDO), is an originally conceived process where the polymer-supported etching and transfer techniques, usually applied to TMD[17] and graphene,[18,19] have been adapted to encapsulated silicene to facilitate its transfer to a target substrate and promptly enable functional applications of the Xene in point. Similar to the SEDNE cases, this approach starts with the disassembling of silicene from the mica slab, but in the t-UXEDO this happens by getting rid of the epitaxial metal substrate, thus allowing not only for the transfer onto arbitrary substrate but also for the possibility to create unprecedented and non-conventional 2D heterostructures, like Xene/TMD heterostructures. Raman spectroscopy has been used to probe the structural integrity of the multilayer silicene through each step of the processes, thus providing compelling evidence of the effectiveness of the presented methodology in developing fabrication steps for Xene integration into functional devices.

2. Results and Discussion

Silicene is grown by molecular beam epitaxy in a UHV chamber system (base pressure 10^{-10} mbar). After growth, the silicene is protected against oxidation by encapsulation, namely the in situ sequential deposition of a 5 nm thick Al_2O_3 capping layer by means of reactive molecular beam deposition. Silicene epitaxy is confirmed in the pre-encapsulation surface morphology by in situ scanning tunneling microscopy analysis and it has been validated by ex situ Raman scattering investigation, as shown in Figure S1, Supporting Information. Further details of the silicene synthesis and characterizations are reported elsewhere.[8]

Figure 1 summarizes the steps of the s-SEDNE approach developed for successive silicene handling. Note that to lend more robustness to the silicene carrying membrane, the pristine 5 nm-thick Al_2O_3 capping layer is further thickened by the deposition of a 50 nm-thick Al_2O_3 by means of atomic layer

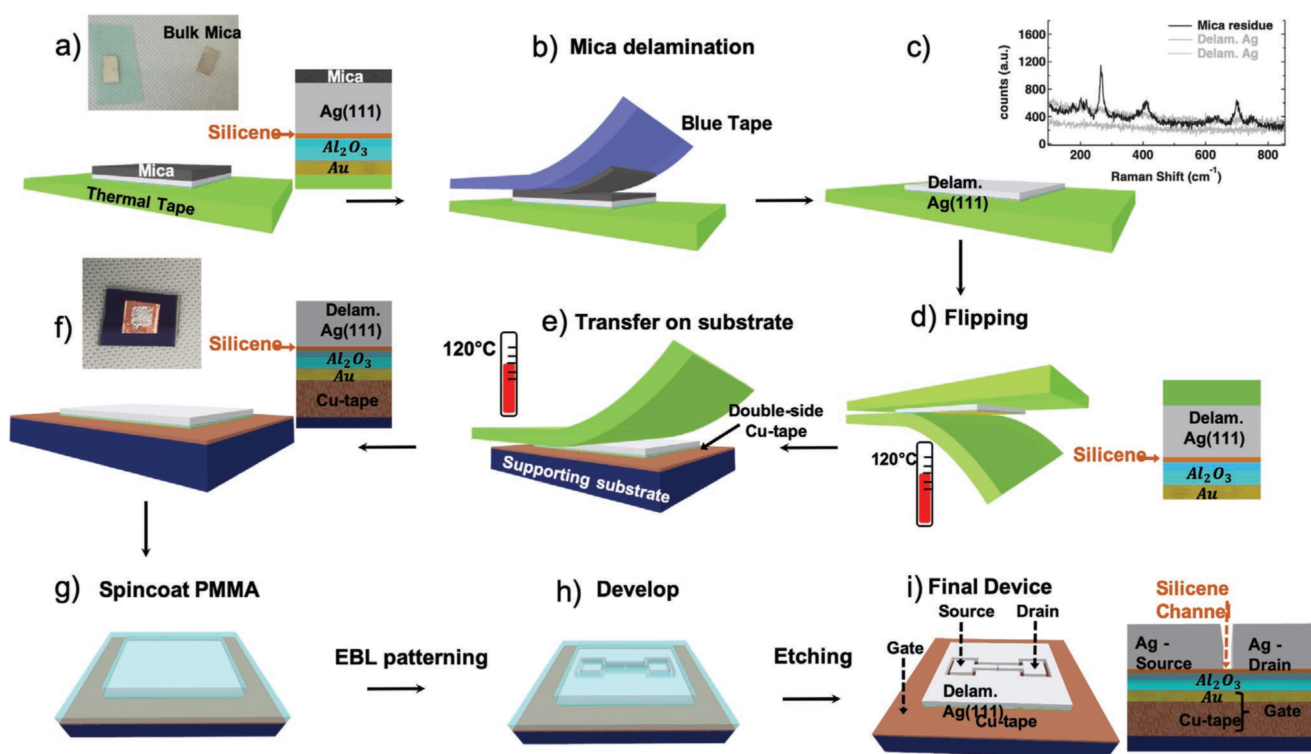

Figure 1. Schematics of the seamless SEDNE process used for the fabrication of a back-gate silicene device. a) After the deposition of a thicker Al_2O_3/Au back-gate the sample is attached, Al_2O_3/Au face-down, to a piece of thermal releasing tape. A big chunk of mica substrate is removed by using another thermal release tape (not shown). b,c) Mechanical delamination of the residual mica layers with blue (Nitto) tape and inspection with Raman spectroscopy of the remaining mica residues on the delaminated Ag-surface. d) Sample flipping. The thermal tape is heated to release the sample from the Al_2O_3/Au side and picked-up with a new piece of thermal tape from the delaminated Ag-side. e,f) Transfer to a new substrate. The sample Al_2O_3/Au face-down is released by heating and attached to a new rigid or flexible supporting substrate with the aid of a double-side copper tape. A back-gate configuration is thus obtained. g,h) PMMA resist spin-coating and EBL definition of the device isolation trenches, channel, and contact-pads. i) The resulting silicene back-gate device structure obtained after the Ag-etching and the PMMA dissolution.

© 2020 The Authors. Published by Wiley-VCH GmbH

deposition and subsequently by the evaporation of an additional 5 nm/100 nm Ti/Au back-gate electrode. Then a piece of thermal release tape (Semiconductor Equipment Corp. single-side coated with releasing temperature of 120 °C) is gently attached on the gate metal (Au) side of the Au/Al_2O_3/silicene/Ag/mica stack (see Figure 1a) applying a uniform pressure to improve the adhesion between the two media. In this way the sample can be turned upside down to exfoliate the thick mica substrate using another piece of thermal release tape leaving only some residual layers of mica (see Figure 1a).The pristine Ag film underlying the thin residual mica layers may readily serve to define electrical contacts on the silicene epitaxial layer with the strong advantage of having no Fermi level misalignment or a chemically-induced barrier at the interface owing to the intrinsic hybridization between Ag and silicene orbitals.[20] However, to have access to the Ag-film, the residual mica layers should be completely stripped off. Given the layered nature of the mica, the most trivial way to do so is delamination by chemical or mechanical means. Mechanically, the delamination can be done either by propagating the stress along the interface with a blade (random process) or by cleaving the layers by scotch tape, the latter being more reliable and controlled as evident from the mechanical exfoliation of van der Waals crystals.[21] The residual mica layers can be completely removed by tape assisted delamination using a 3M blue (Nitto) tape, Figure 1b. The complete removal of the mica layers requires multiple tape peelings. After each step the sample is checked under the Raman microscope to verify the presence of residual mica sheets, see Figure 1c. This peel-off is critical to achieve a smooth and clean surface of silver, as under peel-off will have incomplete mica removal creating huge contact resistance and over peel-off will cause silver surface deformation yielding a high density of wrinkles caused by the release of strain into the metal film. Therefore, an optimum number of peeling is necessary to obtain a large flat surface of silver without any wrinkles. With our optimum number of peelings (≈6–8), flat surfaces of the order of 300–400 μm can be achieved as shown in Figure S2, Supporting Information.

In order to transfer the encapsulated silicene onto a target substrate, the sample orientation must be changed so that the Au side can be attached to the target substrate. This is done by heating the material stack carrying thermal tape on a hot plate for 10 s at 120 °C, in order to loosen its adhesion while another piece of fresh thermal tape is brought in contact to pick the Au/Al_2O_3/silicene/Ag stack from the Ag side (Figure 1d). The stack (Au face-down) is then attached on a double-sided conductive copper tape sitting on an arbitrary (rigid or flexible) substrate and the thermal tape is peeled-off gently by heating it for few seconds at 120 °C (Figure 1e). Due to the stronger adhesion of the copper tape, the Au/Al_2O_3/silicene/Ag stack is left on it with the delaminated Ag film facing up (Figure 1f).

Once the Ag surface is exposed, the sample is further processed by means of a Raith Eline plus electron beam lithography (EBL) facility in order to pattern the device geometry in a 220 nm thick poly (methyl methacrylate) (PMMA) resist spin-coated on the sample, Figure 1g,h. The typical dimensions of a single device area are 200 × 50 μm, but further extreme downscaling to sub tens of nanometers is also possible by optimizing the lithographic step process. After the EBL writing in PMMA, a key step is the definition of the pattern features (contact pads, channels, etc.) into the native Ag film without attacking the silicene underneath it. This step consists of chemical etching of the Ag film through the PMMA mask in order to obtain the device structure schematically depicted in Figure 1i. We observed that commercial Ag etchants based on nitric acid strongly attack silicene and, moreover, are too fast to allow for a reliable definition of the patterned features with a time-controlled etching process. Aqueous solutions of potassium iodide (KI)/Iodine (I_2), however, are better suited for this purpose as they offer selective etching of the Ag film without damaging the underlying silicene. However, commercially available KI/I_2 solutions have typical etching rates of ≈1.2 μm min^{-1} at room-temperature and, therefore, are too fast to achieve a reliable time-controlled etching process on a thin (250 nm) Ag film. Dilution with DI water usually works well to get a reasonably slower etching rate, but we found that it leads to the formation of reaction by-products that are difficult to remove especially while etching 2–5 μm scaled features, see Figure S3, Supporting Information. To tackle this problem, we calibrated the etching rate of in-house KI/I_2 solutions at variable concentrations. We studied their action on Ag test patterns, shown in **Figure 2**a. The etching was performed by dipping the samples into the etchant bath at room-temperature with no agitation, and quenched by careful rinsing in DI water. We found that KI/I_2 solutions in 40 mL pure DI-water at a concentration ratio of $[KI]/[I_2] \approx 3400$ provide reliable etching in terms of pattern resolution without introducing a significant resist undercutting. The topography of the etched Ag has been characterized by atomic force microscopy (AFM), as shown in Figure 2b. For ≈50 μm-scaled features we found that a 250 nm-thick Ag film was completely etched in ≈5 min, as illustrated by the line profile included in Figure 2b. The resulting etching-rate was estimated to be of the order of 40–50 nm min^{-1}. Thin trenches (see Figure 2a), however, were usually etched faster with an observed etching rate 8–9 times higher.

The difference in the etching rate between large and small exposed areas can be detrimental in the nanofabrication of Xene devices. Device channels with small lengths (100–500 nm), can be opened using a quick (<40 s) etching bath. Successive etching steps may help to completely remove the residual Ag from the wide isolation trenches. However, due to the isotropy of the wet etching process, this approach can possibly introduce extensive undercutting along the already etched channel. This issue can be tackled by adopting a two-step strategy in the nanofabrication process. In the first step only the isolation trenches of the source/drain contact-pads are EBL defined and etched by means of a fast commercial iodine/potassium iodide etchant. In the second step the thin channel regions between the source and drain contacts are EBL written and then carefully opened by etching with the slower home-made iodine/potassium iodide etchant. Introducing a slow and time-controlled etching step after the EBL patterning of the device channels allows us to gain a precise definition of these regions that are crucial for the proper functioning of the silicene device. In order to check the survival of the exposed silicene against exposure to our home-made etchant, we defined a device structure with a channel length of ≈1.2 μm, illustrated in Figure 2c). This structure allowed us to have easy access to the laser-probe for

 © 2020 The Authors. Published by Wiley-VCH GmbH

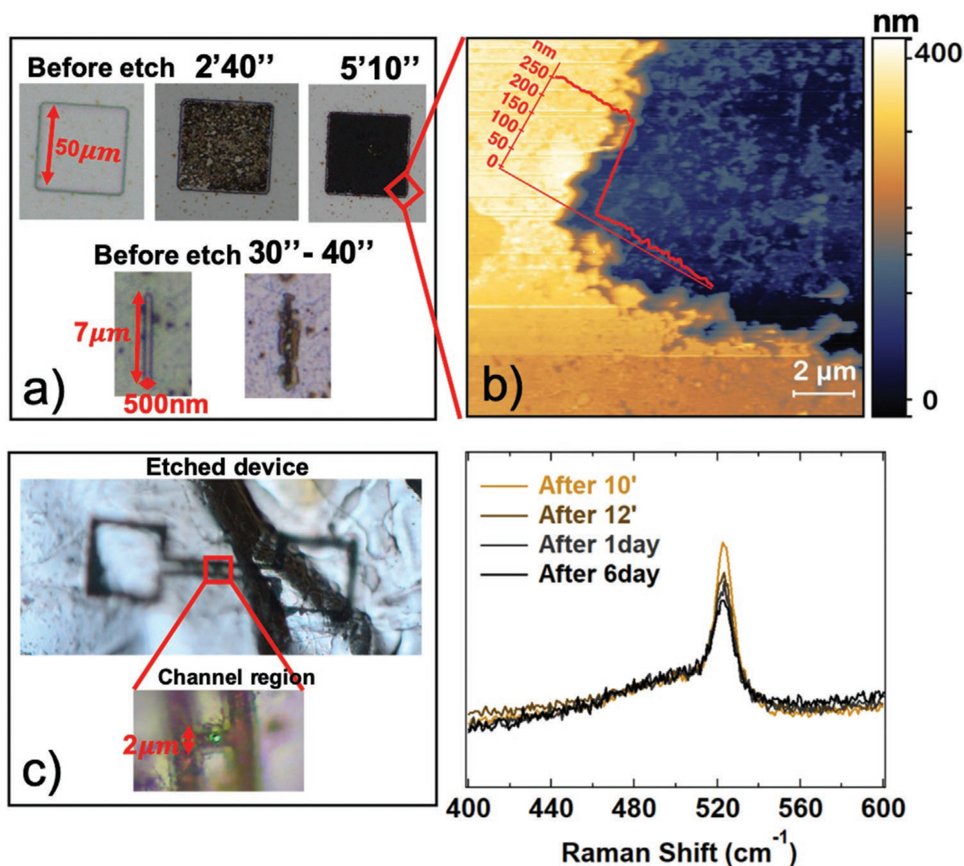

Figure 2. a) Optical microscope images of the Ag-etching on patterns with different size. b) AFM image of the etched region shown in (a) with a superimposed line profile along an etched step. c) Optical microscope image of an etched device structure on a non-planar Ag-film used to verify the stability of the exposed silicene in the etched channel region. The typical device dimensions are 200 × 50 µm. The 1.2 µm wide channel region is highlighted in the close-up image. d) Comparison between the Raman spectra taken after the etching of the channel region shown in (c) after 10 min, 12 min, 1 day, and 6 days of ambient-air exposure and the Raman spectrum of the as-deposited Al_2O_3 capped silicene sample.

Raman spectroscopy in the etched channel region, as shown in the close-up image of Figure 2c. Figure 2d clearly reports that the Raman spectra measured in this region after the etching process after 10–12 min, 1 day and 6 days of ambient-air exposure, all matched well with the spectrum of the as-deposited Al_2O_3-capped silicene samples; thus validating the integrity of the epitaxial layer after delamination, transfer, and device-fabrication process.

Figure 3 summarizes the steps of the t-UXEDO approach as alternative to the handling of the encapsulated Xene. Again, silicene is taken as a crosscheck material. This process consists in a lift-off approach for the separation of the layers from the metal substrate. In detail, we adapted the polymer-supported etching and transferring techniques, developed for TMD[17] and graphene layers,[18,19] to suit our configuration. A film of PMMA (MicroChem, 950 000 MW, 9–6 wt% in anisole) is spin-coated on the encapsulated multilayer silicene, Figure 3a. Afterward, the detachment of the PMMA/Al_2O_3/silicene from metal is obtained by immersion in a commercial Ag etchant solution (based on KI, I_2), Figure 3c. The complete etching of the metal films occurs in several hours. Nevertheless, the etching process is stopped some minutes before the complete release of the PMMA/Al_2O_3/silicene membrane by placing the sample in de-ionized water. This step not only allows us to remove the residues of the etchant solution but also hinders the folding of the membrane once detached from the mica substrate. In the water bath, the release of the mica substrate is obtained by gently favoring the mechanical detachment of the membrane at the edges. It is worth noting that, even though the silver metal film is sacrificed during the etching process, this method allows for the underlying host mica substrate to be recycled. After the mica detachment, the PMMA/Al_2O_3/silicene stack floats on the water surface and can be transferred to an arbitrary target substrate by fishing the membrane with it or, using a colander, letting the membrane ease down on the substrate placed on the bottom of the colander, see Figure S4, Supporting Information. Eventually, the PMMA membrane is dissolved by means of acetone or toluene.

The potential of the t-UXEDO approach as universal transfer scheme is demonstrated by the case of the encapsulated silicene transfer to two different substrates: i) commercial indium tin oxide (ITO), ii) few-layers molybdenum disulfide (MoS_2) grown by chemical vapor deposition on sapphire substrate.[22,23] Proving the transfer in the two cases opens up new directions in nanotechnology. The former substrate is a standard for optoelectronic and energy applications where a transparent

© 2020 The Authors. Published by Wiley-VCH GmbH

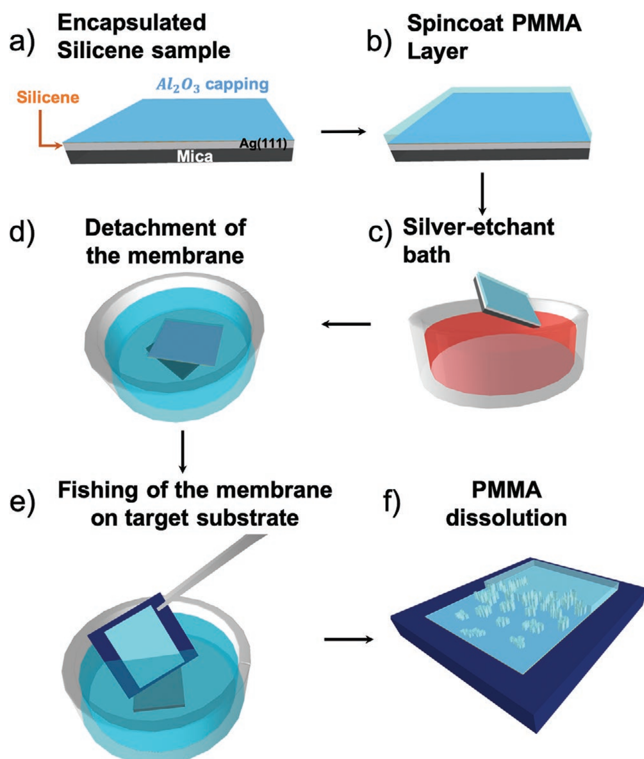

Figure 3. Schematics of the t-UXEDO process. a,b) A PMMA polymer layer is spin-coated on top of the encapsulated silicene. c) The sample is immersed in a commercial KI/I_2 silver etchant solution. d) Before the complete etching of the metallic Ag-film, the sample is immersed in a deionized water bath for the mica detachment. e) The $PMMA/Al_2O_3$/silicene membrane is transferred onto an arbitrary substrate. f) The PMMA layer is finally dissolved by means of acetone or toluene.

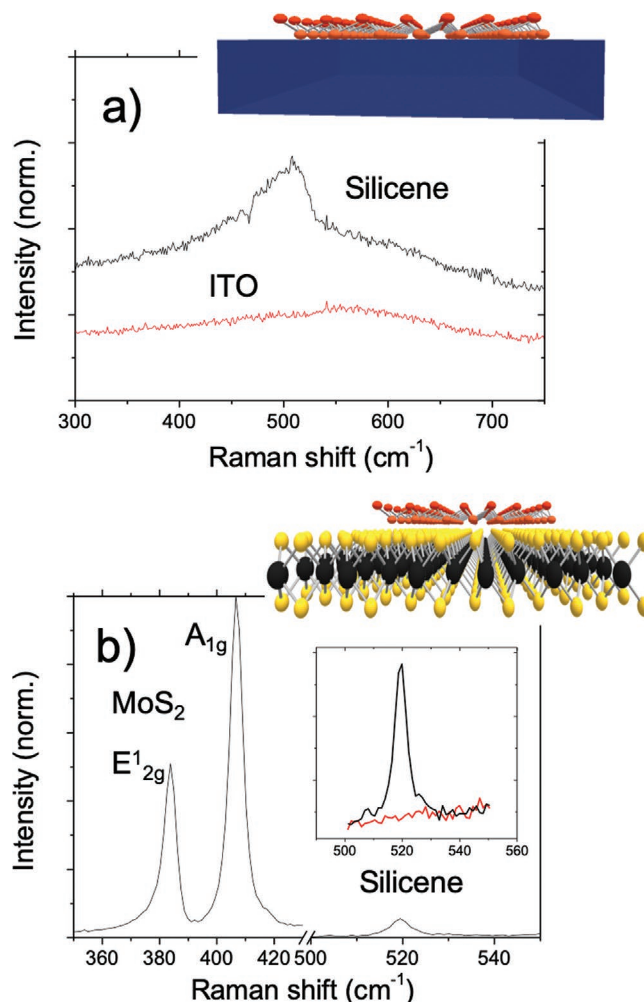

Figure 4. a) Comparison between the Raman spectra of the target ITO substrate (red) and the spectrum measured after the t-UXEDO process. b) Raman spectra of the 4-layers MoS_2/silicene heterostructure. Inset: comparison of the Raman spectra before (red) and after (black) the t-UXEDO process.

electrical contact is required,[24] thus enabling exploitation of Xenes in photovoltaic solar cells or light emitting diode. On the other hand, the latter substrate is the most representative case[25] among the class of the 2D TMDs that may serve as a background to designing new, non-conventional Xene-based heterostructures. The effectiveness of the transfer was probed by Raman spectroscopy, **Figure 4**. As expected, in both sample we observe a Raman peak at wavevector ≈520–523 cm^{-1} which is absent in the spectra of the target substrates before the process (red traces). The detected Raman peak matches with previously reported spectral mode of 2D silicene.[16,26–29] This fact is a compelling evidence of the silicene integrity after transfer.

Figure 4b also shows the characteristic Raman peaks of the MoS_2/sapphire substrate. Notably, the frequency peak separation between the E^1_{2g} and A_{1g} modes of MoS2 is ≈24 cm^{-1}, corresponding to the thickness of four monolayers. This fact demonstrates that we obtained a true all-2D heterostructure made of MoS_2 four layers and silicene, and supported by a sapphire slab, which is in turn an enabling substrate for opto-electronics application. The method is not limited to the materials in use, and by permutation with other members in the TMD and Xene family, in perspective we will be able to fabricate Xene heterostructure by design. A few more remarks are worth being emphasized. First, silicene comes with his protecting encapsulation layer, thus allowing for long-term stability against ageing and air-degradation as confirmed by the Raman peaks that remain unaffected after months. Second, the t-UXEDO is applicable to all the Xenes that are templated by metals and supported by mica, thus paving the way for a number of other Xenes (like borophene, germanene, stanene, etc.) that are momentarily realized at the lab stage with no proven transfer. As a final remark, we note that, avoiding mechanical delamination, strain release is reduced during the transfer, thus allowing a seamless contact area between the multilayer silicene and the hosting substrate. Nevertheless, in contrast with the previously reported s-SEDNE, we found out that the major drawback of this approach is the size of the transferred silicene domains that can be roughly estimated in the μm^2 range.

3. Conclusion

In conclusion, we reported on two handling processes for improving portability and reliability of silicene transfer and

© 2020 The Authors. Published by Wiley-VCH GmbH

device fabrication process. The first approach is a modification of the pristine SEDNE approach, where an additional high-k Al_2O_3 layer and Ti/Au metal electrode is deposited onto the capped multilayer not only to favor the handling of silicene over relatively large-areas (mm^2), but also to provide a seamless dielectric interface in a back gated device configuration. In the second approach, so called t-UXEDO, the epitaxial silicene is completely detached from the metal substrate and transferred onto arbitrary substrates, thus allowing formation of multi-stack configuration. As a result, we were able to demonstrate successful transfer of silicene onto ITO and MoS_2 substrates. Notably, the latter case constitutes the first example of an assembly of a fully 2D Xene-based heterostructure. Raman spectroscopy probed the structural integrity of the encapsulated multilayer silicene through each step of the processes, thus providing compelling evidence of the effectiveness of the presented methodologies in developing universal fabrication schemes for Xene integration into functional devices and substrates.

Supporting Information

Supporting Information is available from the Wiley Online Library or from the author.

Acknowledgements

C.M. and G.F. contributed equally to this work. Otitoaleke ‘Leke Akinola, Michael Rodder, and Mario Alia are acknowledged for technical support. A.M. acknowledges EU funding from the H2020 research and innovation programme under the ERC-COG 2017 grant no. 772261 “XFab.”

Conflict of Interest

The authors declare no conflict of interest.

Keywords

2D materials, processing, silicene, transfer, Xenes

Received: May 27, 2020
Revised: June 19, 2020
Published online:

[1] A. Molle, J. Goldberger, M. Houssa, Y. Xu, S.-C. Zhang, D. Akinwande, *Nat. Mater.* **2017**, *16*, 163.
[2] D. Akinwande, N. Petrone, J. Hone, *Nat. Commun.* **2014**, *5*, 5678.
[3] G. Fiori, F. Bonaccorso, G. Iannaccone, T. Palacios, D. Neumaier, A. Seabaugh, S. K. Banerjee, L. Colombo, *Nat. Nanotechnol.* **2014**, *9*, 768.
[4] A. C. Ferrari, F. Bonaccorso, V. Fal’ko, K. S. Novoselov, S. Roche, P. Bøggild, S. Borini, F. H. L. Koppens, V. Palermo, N. Pugno, J. A. Garrido, R. Sordan, A. Bianco, L. Ballerini, M. Prato, E. Lidorikis, J. Kivioja, C. Marinelli, T. Ryhänen, A. Morpurgo, J. N. Coleman, V. Nicolosi, L. Colombo, A. Fert, M. Garcia-Hernandez, A. Bachtold, G. F. Schneider, F. Guinea, C. Dekker, M. Barbone, et al., *Nanoscale* **2015**, *7*, 4598.
[5] C. Grazianetti, C. Martella, A. Molle, *Phys. Status Solidi RRL* **2020**, *14*, 1900439.
[6] A. Molle, C. Grazianetti, L. Tao, D. Taneja, M. H. Alam, D. Akinwande, *Chem. Soc. Rev.* **2018**, *47*, 6370.
[7] L. Tao, E. Cinquanta, D. Chiappe, C. Grazianetti, M. Fanciulli, M. Dubey, A. Molle, D. Akinwande, *Nat. Nanotechnol.* **2015**, *10*, 227.
[8] A. Molle, G. Faraone, A. Lamperti, D. Chiappe, E. Cinquanta, C. Martella, E. Bonera, E. Scalise, C. Grazianetti, *Faraday Discuss.* **2020**, https://doi.org/10.1039/c9fd00121b.
[9] E. S. Walker, S. R. Na, D. Jung, S. D. March, J. S. Kim, T. Trivedi, W. Li, L. Tao, M. L. Lee, K. M. Liechti, D. Akinwande, S. R. Bank, *Nano Lett.* **2016**, *16*, 6931.
[10] P. Vogt, P. de Padova, C. Quaresima, J. Avila, E. Frantzeskakis, M. C. Asensio, A. Resta, B. Ealet, G. le Lay, *Phys. Rev. Lett.* **2012**, *108*, 155501.
[11] J. L. Zhang, S. Zhao, C. Han, Z. Wang, S. Zhong, S. Sun, R. Guo, X. Zhou, C. D. Gu, K. di Yuan, Z. Li, W. Chen, *Nano Lett.* **2016**, *16*, 4903.
[12] M. E. Dávila, L. Xian, S. Cahangirov, A. Rubio, G. le Lay, *New J. Phys.* **2014**, *16*, 095002.
[13] Y. Shao, Z.-L. Liu, C. Cheng, X. Wu, H. Liu, C. Liu, J.-O. Wang, S.-Y. Zhu, Y.-Q. Wang, D.-X. Shi, K. Ibrahim, J.-T. Sun, Y.-L. Wang, H.-J. Gao, *Nano Lett.* **2018**, *18*, 2133.
[14] J. Deng, B. Xia, X. Ma, H. Chen, H. Shan, X. Zhai, B. Li, A. Zhao, Y. Xu, W. Duan, S.-C. Zhang, B. Wang, J. G. Hou, *Nat. Mater.* **2018**, *17*, 1081.
[15] C. Grazianetti, G. Faraone, C. Martella, E. Bonera, A. Molle, *Nanoscale* **2019**, *11*, 18232.
[16] C. Grazianetti, E. Cinquanta, L. Tao, P. de Padova, C. Quaresima, C. Ottaviani, D. Akinwande, A. Molle, *ACS Nano* **2017**, *11*, 3376.
[17] J. Shi, D. Ma, G. F. Han, Y. Zhang, Q. Ji, T. Gao, J. Sun, X. Song, C. Li, Y. Zhang, X. Y. Lang, Y. Zhang, Z. Liu, *ACS Nano* **2014**, *8*, 10196.
[18] J. Kang, D. Shin, S. Bae, B. H. Hong, *Nanoscale* **2012**, *4*, 5527.
[19] A. Reina, H. Son, L. Jiao, B. Fan, M. S. Dresselhaus, Z. F. Liu, J. Kong, *J. Phys. Chem. C* **2008**, *112*, 17741.
[20] D. Tsoutsou, E. Xenogiannopoulou, E. Golias, P. Tsipas, A. Dimoulas, *Appl. Phys. Lett.* **2013**, *103*, 231604.
[21] H. Li, G. Lu, Y. Wang, Z. Yin, C. Cong, Q. He, L. Wang, F. Ding, T. Yu, H. Zhang, *Small* **2013**, *9*, 1974.
[22] S. Vangelista, E. Cinquanta, C. Martella, M. Alia, M. Longo, A. Lamperti, R. Mantovan, F. B. Basset, F. Pezzoli, A. Molle, *Nanotechnology* **2016**, *27*, 175703.
[23] C. Martella, P. Melloni, E. Cinquanta, E. Cianci, M. Alia, M. Longo, A. Lamperti, S. Vangelista, M. Fanciulli, A. Molle, *Adv. Electron. Mater.* **2016**, *2*, 1600330.
[24] M. A. Green, *J. Mater. Sci. Mater. Electron.* **2007**, *18*, 15.
[25] M. Chhowalla, H. S. Shin, G. Eda, L.-J. Li, K. P. Loh, H. Zhang, *Nat. Chem.* **2013**, *5*, 263.
[26] J. Zhuang, X. Xu, Y. Du, K. Wu, L. Chen, W. Hao, J. Wang, W. K. Yeoh, X. Wang, S. X. Dou, *Phys. Rev. B: Condens. Matter Mater. Phys.* **2015**, *91*, 161409.
[27] S. Sheng, J. Bin Wu, X. Cong, W. Li, J. Gou, Q. Zhong, P. Cheng, P. H. Tan, L. Chen, K. Wu, *Phys. Rev. Lett.* **2017**, *119*, 196803.
[28] Y. Du, J. Zhuang, J. Wang, Z. Li, H. Liu, J. Zhao, X. Xu, H. Feng, L. Chen, K. Wu, X. Wang, S. X. Dou, *Sci. Adv.* **2016**, *2*, e1600067.
[29] E. Cinquanta, E. Scalise, D. Chiappe, C. Grazianetti, B. van den Broek, M. Houssa, M. Fanciulli, A. Molle, *J. Phys. Chem. C* **2013**, *117*, 16719.

© 2020 The Authors. Published by Wiley-VCH GmbH